MINISTÉRIO DA CIÊNCIA E TECNOLOGIA
INSTITUTO DE PESQUISAS ESPACIAIS

AUTORIZAÇÃO PARA PUBLICAÇÃO
AUTHORIZATION FOR PUBLICATION

PALAVRAS CHAVES/KEY WORDS — AUTORES/AUTHORS

STARS: BINARIES
ULTRAVIOLET: SPECTRA
STARS: INDIVIDUAL (BE UMa)
STAR: WHITE DWARFS

AUTORIZADA POR/AUTHORIZED BY

Marco Antonio Raupp
1º Diretor-Geral

AUTOR RESPONSÁVEL / RESPONSIBLE AUTHOR

João E. Steiner

DISTRIBUIÇÃO/DISTRIBUTION

- [ ] INTERNA / INTERNAL
- [x] EXTERNA / EXTERNAL
- [ ] RESTRITA / RESTRICTED

REVISADA POR / REVISED BY

Hugo V. Capelato

CDU/UDC

523.851.4

DATA / DATE

September 1987

PUBLICAÇÃO Nº / PUBLICATION NO

INPE-4348-PRE/1184

ORIGEM / ORIGIN

CEA

PROJETO / PROJECT

ASTRO

Nº DE PAG. / NO OF PAGES

12

ÚLTIMA PAG. / LAST PAGE

12

VERSÃO / VERSION

Nº DE MAPAS / NO OF MAPS

TÍTULO/TITLE

BE URSAE MAJORIS: A DETACHED BINARY WITH A UNIQUE REPROCESSING SPECTRUM

IN-74
120104
NASA-CR

GODDARD GRANT

AUTORES/AUTHORSHIP

Donald H. Ferguson
James Liebert
Roc Cutri
Ricard F. Green
S. P. Willner
João E. Steiner
Susan Tokarz

RESUMO-NOTAS/ABSTRACT-NOTES

A variety of new observations are presented of the unusual detached binary system BE UMa. These include new infrared photometry, optical and ultraviolet spectrophotometry, and a photographic ephemeris. The new information is used to model the systemic and stellar parameters and to analyze the reprocessing spectrum in the secondary.

OBSERVAÇÕES/REMARKS

Trabalho publicado na The Astrophysical Journal - 316:399-410, 1987 - May 1.

BE URSAE MAJORIS: A DETACHED BINARY WITH A UNIQUE REPROCESSING SPECTRUM[1]

DONALD H. FERGUSON,[2,3] JAMES LIEBERT,[3] AND ROC CUTRI
Steward Observatory, University of Arizona
RICHARD F. GREEN[3]
Kitt Peak National Observatory, National Optical Astronomy Observatories[4]
AND
S. P. WILLNER, JOÃO E. STEINER,[5] AND SUSAN TOKARZ
Harvard-Smithsonian Center for Astrophysics
Received 1986 July 22; accepted 1986 October 22

ABSTRACT

A variety of new observations are presented of the unusual detached binary system BE UMa. These include new infrared photometry, optical and ultraviolet spectrophotometry, and a photographic ephemeris. The new information is used to model the systemic and stellar parameters and to analyze the reprocessing spectrum in the secondary.

Higher resolution optical spectroscopy reveals that the primary is a DO white dwarf showing He II lines and a trace of hydrogen. There is no indication in these data that this component is a photometric or spectroscopic variable star. Parameters derived from atmospheric modeling suggest $T_p = 80{,}000 \pm 15{,}000$ K and $7.0 < \log g_p < 8.0$. The inferred mass is $0.6 \pm 0.1\ M_\odot$. This component dominates the energy distribution from the ultraviolet to 1 μm at minimum light outside eclipse. Spectrophotometry dominated by the secondary star during eclipse shows this component to be an M1–M5 dwarf, with no indication that its parameters deviate substantially from those of a normal main-sequence star. Photometric parallaxes derived from both components agree on a best distance estimate of ~ 600 pc.

EUV radiation from the hot primary incident on the secondary atmosphere produces a spectacular "reflection effect" in reprocessed line and continuum radiation. The temperature of the reprocessed component of the secondary's atmosphere is probably in the range $5000 < T_{rep} < 8500$ K. Emission lines of decreasing ionization form deeper in the irradiated envelope. He II and high-excitation metal lines (such as the C III λ4650 components) appear relatively narrow and are formed from recombination and continuum fluorescence processes. The breadths and flat decrement of the hydrogen and He I lines suggest formation at $T_e > 10{,}000$ K and $n_e \approx 10^{14}$ cm^{-3}. Finally, we contrast BE UMa with the similar detached binaries Feige 24 and GK Vir, which also have very hot white dwarf primary stars.

Subject headings: stars: binaries — stars: individual (BE UMa) — stars: white dwarfs — ultraviolet: spectra

I. INTRODUCTION

BE Ursae Majoris is an apparently detached, eclipsing binary system with very unusual properties. Although previously known as a periodic variable (Kurochkin 1964, 1971), the object was rediscovered as a blue, stellar object with an unusual, variable emission-line spectrum (Ferguson *et al.* 1981, hereafter Paper I) strongly modulated with the 2.29 day binary period (Margon, Downes, and Katz 1981, hereafter MDK). Since the primary star is extremely hot (T_{eff} of order 10^5 K), its ultraviolet flux impinging on the facing surface of the cool secondary produces the unusual emission-line spectrum and the dominant optical continuum radiation. Both of these are maximal when the secondary is behind the white dwarf in the observer's line of sight. Conversely, these components nearly disappear when the secondary nears inferior conjunction with the hot primary dominating the spectrum at optical wavelengths, as it always does in the ultraviolet. Ando, Okazaki, and Nishimura (1982, hereafter AON) discovered that a 1 mag eclipse actually occurs at inferior conjunction, punctuating the minimum light phase of the otherwise sinusoidal optical light curve.

The emission-line spectrum of BE UMa away from minimum light shows an uncanny resemblance to those of some high-excitation cataclysmic variables, except that the lines are much narrower (Paper I). The spectra exhibit a flat Balmer decrement, a large Balmer jump in emission, strong He II λ4686 and C III λ4650, a flat decrement of He I lines with similar singlet and triplet line strengths, and still weaker high-excitation lines due to other ions. The optical continuum component due to reprocessing is quite flat: $f_\nu \propto \nu^0$ over $\lambda\lambda$3300–9000, but ultraviolet spectra with the *International Ultraviolet Explorer* (*IUE*) observatory showed a sharp upturn proportional to ν^{+1} over $\lambda\lambda$1200–3000. The appearance of He II absorption in both the *IUE* spectrum and an optical

[1] This research used in part the facilities of the Multiple Mirror Telescope Observatory, operated by the Harvard-Smithsonian Center for Astrophysics and the University of Arizona; observations were also done at the Palomar Observatory, operated by the California Institute of Technology.

[2] Current address: Lockheed Missiles and Space Company, Inc., Sunnyvale, California.

[3] Guest Investigator, *International Ultraviolet Explorer* telescope, operated by NASA at the Goddard Space Flight Center, Greenbelt, Maryland.

[4] Operated by the Association of Universities for Research in Astronomy, Inc., under contract with the National Science Foundation.

[5] Current address: Instituto de Pesquisas Espaciais, São Jose dos Campos, S.P., Brazil.

spectrum near minimum light (Paper I) also implied a very hot, evolved primary star with a helium-rich composition.

MDK obtained spectra over several consective nights and showed that the emission lines varied with the photometric phase. They identified the BE UMa primary as a hot white dwarf and argued that a secondary star of mass less than 0.4 $M_\odot$ would be consistent with the small contribution to the flux in the visible. From the radial separation implied by the assumed masses, they estimated that $\sim 10^{-3}$ of the primary's radiation impinges on the secondary star, implying a bolometric correction of ~ -7.5 mag and a primary temperature of order 10^5 K.

Ferguson (1983) confirmed the binary nature of BE UMa by finding radial velocity variations in three emission lines, consistent with an orbital semiamplitude of the emission component $K_2 \sin i = 95 \pm 7$ km s^{-1}. However, the Hβ λ4861, He II λ4686, and C III λ4650 lines displayed different velocity profiles; details are discussed in § IV*b*. Crampton, Cowley, and Hutchings (1983, hereafter CCH) have improved radial velocity data, showing a mean $K_2 \sin i = 103 \pm 2$ km s^{-1} and a mean velocity of -67 ± 2 km s^{-1}.

AON found the eclipse in five-color photoelectric photometry; it lasts 72 ± 2 minutes centered on the minimum of the sinusoidal variation. The drop in U was ~ 5 mag and showed a V shape lacking a flat minimum; yet the drop in V was ~ 1.5 mag and exhibited a rounder U shape. They used Ferguson's (1981) $K_2 \sin i$ to estimate the mass function $f(m) = 0.204\ M_\odot$. Invoking the mass-radius relation for main-sequence stars, they found $0.10 \leq R_p/R_\odot \leq 0.15$ and $0.5 \leq M_p/M_\odot \leq 0.8$. Using the mass-luminosity relations for helium-rich stars of Cox and Giuli (1961), they suggested that the primary is a helium-rich, subdwarf O star with $4 \leq T_p/10^4\ \mathrm{K} \leq 6$.

CCH used extensive time-resolved spectroscopy and the light curves of AON to reexamine the physical parameters of the system. From their radial velocity curve, they derived a mass function $f(m) = 0.25\ M_\odot$. They interpreted the flat-bottomed photoelectric V curve as measuring the time of total eclipse of the primary by the secondary. Using Ferguson's (1983) estimated spectral type of the secondary during eclipse of M2 V, these authors deduced (1) that the secondary's radius must exceed the main-sequence value, and (2) that the ratio of the amplitude of the reprocessed component in the light curve to the eclipse depth required a very small, hot primary star. Quantitatively, they derived $T_p \approx 130{,}000$ K and $R_p = 0.028 \pm 0.008\ R_\odot$, appropriate to the gravity of a borderline white dwarf/subdwarf. However Hutchings and Cowley (1985) now report some strange variations in *IUE* ultraviolet spectrophotometry and suggest that the primary star may be related to the PG 1159 – 035 class of pulsating variables.

In this paper, we present in § II a variety of new data: First, the photographic data base is given from which the current ephemeris (CCH) has been derived. High-dispersion line profile data are discussed. Then, we present ultraviolet, optical, and infrared flux measurements at various binary phases. Moderate-dispersion spectra near minimum light allow analysis of the photospheres of the primary and the unilluminated secondary stars. In § III, we reanalyze the parameters of both components in the BE UMa system. Section IV presents a discussion of the emission-line diagnostics in the reprocessing spectrum. Some of these results were also presented in the Ph.D. thesis of Ferguson (1983).

II. NEW OBSERVATIONS

The following sections summarize a variety of data on the BE UMa system obtained since Paper I; some of these results were discussed by Ferguson (1983). Table 1 is a summary of all new observations.

a) The Ephemeris

Using the Harvard plate data discussed by Ferguson (1983), CCH found the ephemeris centered on minimum light to be HJD 2,444,998.281 + 2.291171E days. This is currently the best available and is used throughout this paper when referring to the phasing of observations. Figure 1 and Table 2 present the complete Harvard plate data, with magnitudes estimated by the technique of Liller and Liller (1975), together with more recent data from Kurochkin (1971). With the exception of several data points near phase 0 in the historical data where

TABLE 1

SUMMARY OF SPECTROSCOPIC OBSERVATIONS OF BE URSAE MAJORIS

Date (UT)	Instrument	Wavelength Coverage (Å)	Resolution (Å)	Exposure (minutes)	Phase
1981 Jan 9, 10	Mb	5100–6600	4	60	0.21, 0.25
1981 Jan 10	Mb	4250–4900	2	88	0.14
1981 Feb 2	Mb	4250–4900	2	40	0.75
1981 Feb 11	I	1100–1900	6	40	0.15
1981 Apr 7	Sr	5300–8700	15	15	0.96
1981 Apr 11	Sr	5300–8700	15	15	0.35
1981 May 9	H	3100–11000	80	12	0.56
1981 May 10	H	3100–11000	80	12	0.98
1981 May 11	H	3100–11000	80	12	0.55
1981 May 10	Mb	4430–4930	3	36	0.98
1981 May 11	I	1100–1900	6	60	0.41
1981 Jun 20–23	Me	4650, 4686, 4861	0.2	...	0.84, 0.27 0.71, 0.15
1982 Jan 24	Mb	4300–4900	5	40	0.02
		5200–5600	3	30	0.03
1982 Mar 4	Sb	3200–7000	15	12	0.00

INSTRUMENT.—Mb: MMT, Cassegrain spectrograph, blue Reticon. I: *IUE*. Sr: Steward 2.3 m, Cassegrain spectrograph, red Reticon. H: Hale 5 m MCSP. Me: MMT, echelle spectrograph. Sb: Steward 2.3 m, Cassegrain spectrograph, blue Reticon.

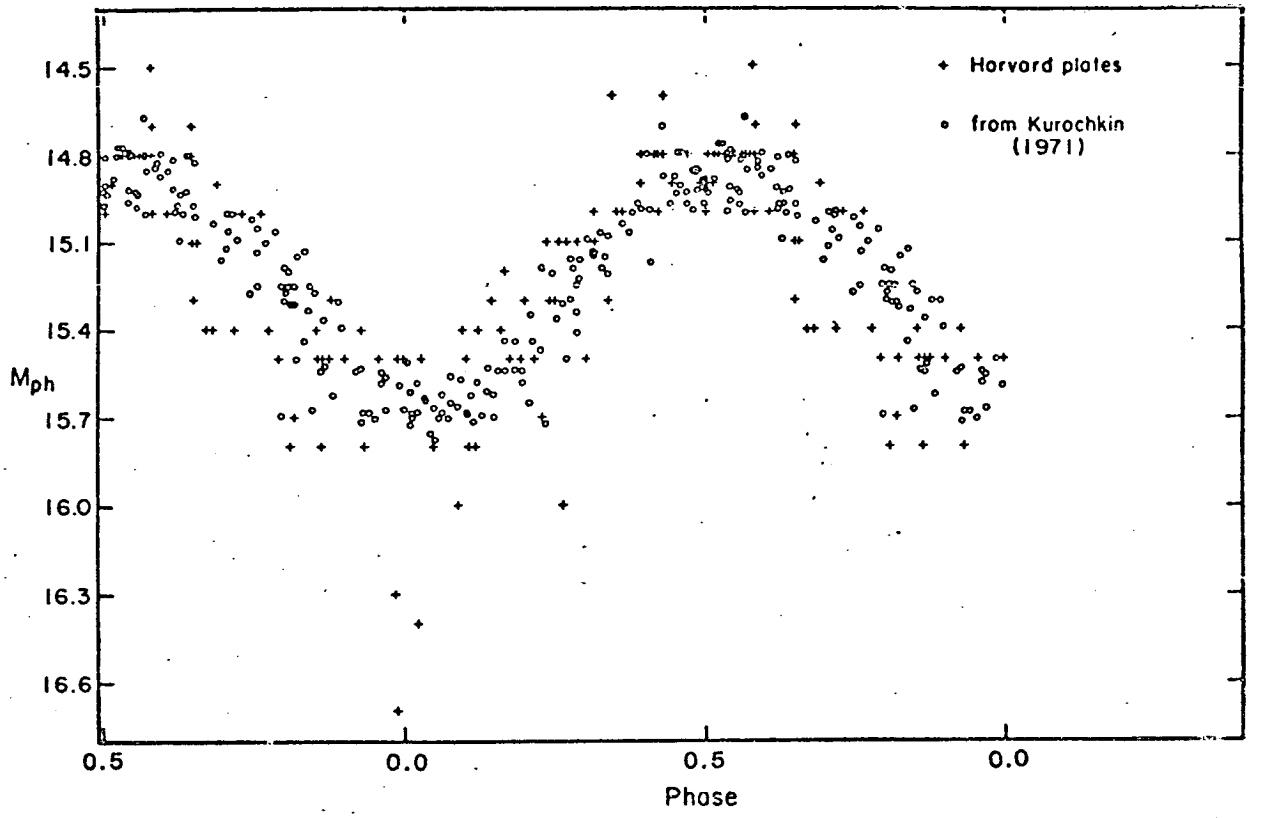

FIG. 1.—Light curve for BE UMa constructed from magnitudes from the Harvard plates (*pluses*) and those taken from Kurochkin (1971; *circles*)

the primary was eclipsed, the data gave an excellent fit to a sine wave. An analysis of the Harvard plates taken between 1889 and 1953 gives no indication of a binary period change, though this would hardly be expected for such a wide, detached binary. Moreover, the data indicate that there is no evidence for long-term variability of the BE UMa system, despite the claim that the secondary may be close to filling its Roche lobe (CCH).

b) Infrared Photometry

Broad-band infrared *JHK* photometry was obtained at several epochs with the facility infrared photometer at the Multiple Mirror Telescope (MMT) and with the Steward Observatory infrared photometer at the Catalina 1.55 m reflector. Both photometer systems utilize liquid helium–cooled InSb photovoltaic detectors. The results of both sets of observations are listed in Table 3.

The MMT photometry used a beam size of 9″ and chopper spacings ranging from 10″ to 13″. At the 1.55 m, measurements were made through a 7.″8 diameter using a chopper offset of 10″. The *H*- and *K*-magnitudes given on the instrumental system in Table 3 closely approximate those on the Caltech system (Elias *et al.* 1982), while the *J*-magnitudes can be approximately converted to the Caltech system via the relation $(J-K)_{CIT} = (J-K)_{\odot}/1.066$. The 1.54 m photometry was made through apertures 7.″8–8.″7 in diameter, with a chopper offset of 10″.

The uncertainties in the MMT observations can be estimated from observations of a nearby field star (BD +49°2101), which was measured just before or after BE UMa on all nights after the first two. The dispersion of the measured field star magnitudes was 0.07 at each of the three wavelengths, and this is a reasonable estimate of the internal uncertainty in most of the measurements. Statistical uncertainties were generally less than 0.04 mag; for the exceptions, Table 3 gives the statistical uncertainty added quadratically to 0.07 mag. One of the main sources of uncertainty in MMT photometry is the gradual separation of the images from the six individual telescopes. This separation was potentially different for the measurements of the field star and of BE UMa, so on most nights it is not appropriate to use the field star as a primary standard. Instead, the measurements of the field star were reduced separately in the same manner as the measurements of BE UMa and compared. Table 3 gives the average of these comparisons for each night in the sense that positive numbers imply that the star was measured to be fainter than normal. On two nights, however, measurements were made through thin clouds, and the field star was used as the primary standard with adopted magnitudes $J = 8.94$, $H = 8.78$, and $K = 8.79$. These two nights are indicated by deviations of 0.0; had regular standard stars been used instead, the deviations would have been 0.04 and 0.10.

One additional source of uncertainty affects only the measurements on the last four lines of Table 3. An electronic problem during this telescope run caused faint objects to be measured as too faint. BE UMa was brighter than the objects for which this problem is known to be significant, but comparison of the observations at phases 0.81 and 0.83 or phases 0.56 and 0.58 suggests that there might be a discrepancy as large as 0.3 mag. On the other hand, the QSO B2 1225+317 is about as bright as BE UMa and was measured at the correct magnitudes on the last two of the four nights in question. These measurements suggest that the error is unlikely to be more than ~0.2 mag on the night that BE UMa was faintest and

TABLE 2

HARVARD PLATE COLLECTION DATA

JD (2,400,000+)	M_B	Phase*	JD (2,400,000+)	M_B	Phase*
11336.894	15.3	0.22	29620.927	14.6	0.43
15016.632	14.6	0.40	29662.856	15.0	0.73
15443.791	15.3	0.71	29676.776	15.8	0.81
16890.855	15.1	0.29	29676.805	15.7	0.82
17301.667	14.8	0.59	29726.572	14.8	0.54
23053.942	15.5	0.22	29730.604	15.5	0.30
25290.813	14.9	0.52	29730.628	15.0	0.31
27391.892	14.8	0.55	29730.737	15.0	0.36
27778.873	14.9	0.45	30049.669	14.8	0.56
27785.885	14.8	0.51	30049.693	14.8	0.57
27806.828	14.8	0.65	30050.735	15.5	0.02
27833.803	14.8	0.43	30052.648	15.8	0.86
27865.815	14.9	0.40	30058.676	14.9	0.49
27887.660	15.4	0.93	30058.699	15.0	0.50
27892.624	15.4	0.10	30088.722	15.0	0.60
27895.682	14.8	0.43	30099.598	15.0	0.35
27896.785	15.5	0.83	30101.605	15.7	0.23
27896.866	15.5	0.86	30106.635	15.0	0.42
27984.656	16.0	0.27	30136.632	14.9	0.51
27985.617	15.4	0.69	30172.591	15.5	0.21
28197.741	14.8	0.52	30368.831	15.5	0.86
28196.905	15.5	0.90	30403.717	16.0	0.09
28217.733	16.7	0.99	30403.767	15.8	0.11
28218.734	14.7	0.43	30410.783	15.5	0.17
28222.705	15.4	0.17	30732.794	15.4	0.71
28222.794	15.3	0.20	30735.780	16.4	0.02
28520.904	15.1	0.32	30758.772	15.7	0.05
28568.867	15.3	0.25	30812.662	14.5	0.57
28576.713	15.4	0.67	31145.833	15.5	0.99
28579.726	16.3	0.99	31493.807	15.5	0.86
28654.573	15.1	0.66	31522.789	14.8	0.51
28878.932	15.0	0.58	31823.871	15.8	0.92
28926.847	14.9	0.49	31877.798	14.8	0.46
28937.787	15.1	0.27	32291.654	15.5	0.09
28956.724	14.8	0.53	32591.840	15.4	0.11
28985.656	15.1	0.29	32640.636	14.8	0.41
28985.667	15.2	0.17	32890.898	15.1	0.64
28990.647	15.3	0.34	32950.755	15.4	0.76
29315.773	15.3	0.24	32996.758	15.4	0.84
29342.680	15.5	0.99	33023.604	14.8	0.56
29351.772	15.5	0.96	33351.745	15.5	0.78
29395.574	15.7	0.07	33651.820	15.0	0.75
29395.662	15.8	0.11	33763.676	14.7	0.57
29398.603	14.8	0.40	33771.613	15.8	0.03
29400.603	15.5	0.27	34072.841	14.8	0.50
29419.646	14.8	0.58	34093.751	14.7	0.63
			34123.633	14.9	0.67

* Based on T = JD 2,444,998.281, P = 2.291171.

under 0.1 mag on the other three nights. Nevertheless, the measurements on these four nights may be systematically too faint. None of the analysis presented depends on these measurements.

For the following comparison with fluxes at shorter wavelengths, these infrared magnitudes have been converted to monochromatic fluxes using the calibrations given in Neugebauer *et al.* (1979).

c) *The Overall Energy Distribution*

The ultraviolet and optical energy distributions corresponding to phases 0.31 and 0.37 respectively were presented in Paper I. Note that, with the improved ephemeris, these phases differ from those listed in Table 1 of that paper. These and some new ultraviolet and optical fluxes, along with the new infrared *JHK* flux densities, are presented in Figure 2. In particular, Palomar 5 m multichannel spectrophotometry (MCSP) data immediately before eclipse and near maximum light are presented.

Shortward of 2000 Å, there is no evidence for significant variability between phases near optical maximum and minimum. This is consistent with the assumption that a nonvariable primary star dominates this region of the spectrum. Redward of 3000 Å, the energy distribution varies over about a magnitude between minimum and maximum light, as expected. The observations nearest the phase of optical minimum

TABLE 3

INFRARED MAGNITUDES OF BE URSAE MAJORIS

JD (−2,440,000)	Phase	J	H	K	Δ*
		Catalina 1.6 m			
4952.03.....	0.81	14.70	14.22	13.93	...
4953.06.....	0.26	14.30	13.95	13.80	...
4955.06.....	0.14	14.82	14.42	14.24 ± 0.07	−0.05
4956.04.....	0.56	13.82	13.63	13.45	−0.03
		MMT			
5449.89.....	0.11	14.88	14.45	14.40 ± 0.08	0.04
5803.90.....	0.62	13.96	13.71	13.49	0.03
5001.90.....	0.58	14.16	13.67	13.60	0.00
5002.94.....	0.03	15.73 ± 0.09	14.95 ± 0.08	14.79 ± 0.08	0.00
5003.87.....	0.44	13.98	13.73	13.75 ± 0.09	−0.03
5004.78.....	0.83	15.19	14.51	14.38 ± 0.13	0.06

* Average difference between measurements of the field star, presumed to be non-variable, and its average value (see § 11*b*).

confirm the dominance of the hot star well into the optical wavelengths. The same $f_\nu \propto \nu^{+1}$ power law smoothly connects the short-wavelength *IUE* and the phase 0.98 MCSP scan shortward of 5000 Å. There is no evidence in the latter for a Balmer jump in either emission or absorption. Longward of 5000 Å, the MCSP scan is flat at phase 0.98.

At other phases, the optical continuum fits a power law of $\sim\nu^{-0.3}$ redward of the Balmer jump and strongest blue emission lines and is obviously dominated by reprocessing on the secondary star. The long-wavelength camera *IUE* spectrum at phase 0.28 is consistent with the rise of the strong Balmer continuum emission seen in the MCSP energy distribution at phase 0.31/0.37. The MCSP and infrared photometry gathered near phase 0.5 (optical maximum) show that the reprocessed component peaks near 7500 Å. At phases nearer to minimum light, however, the infrared flux is much weaker and shows a peak in the H(1.6 μm) band; nearest minimum light (phase 0.03) the infrared flux levels fall near but significantly above the extrapolated Rayleigh Jeans tail of the primary star, as indicated by the *IUE* and MCSP fluxes.

d) Lower Dispersion Spectroscopy: The Absorption Line Spectra of Both Stellar Components

As shown in the previous section, the optical component due to reprocessing virtually disappears below 5000 Å near the time of eclipse. This made possible study of the primary star

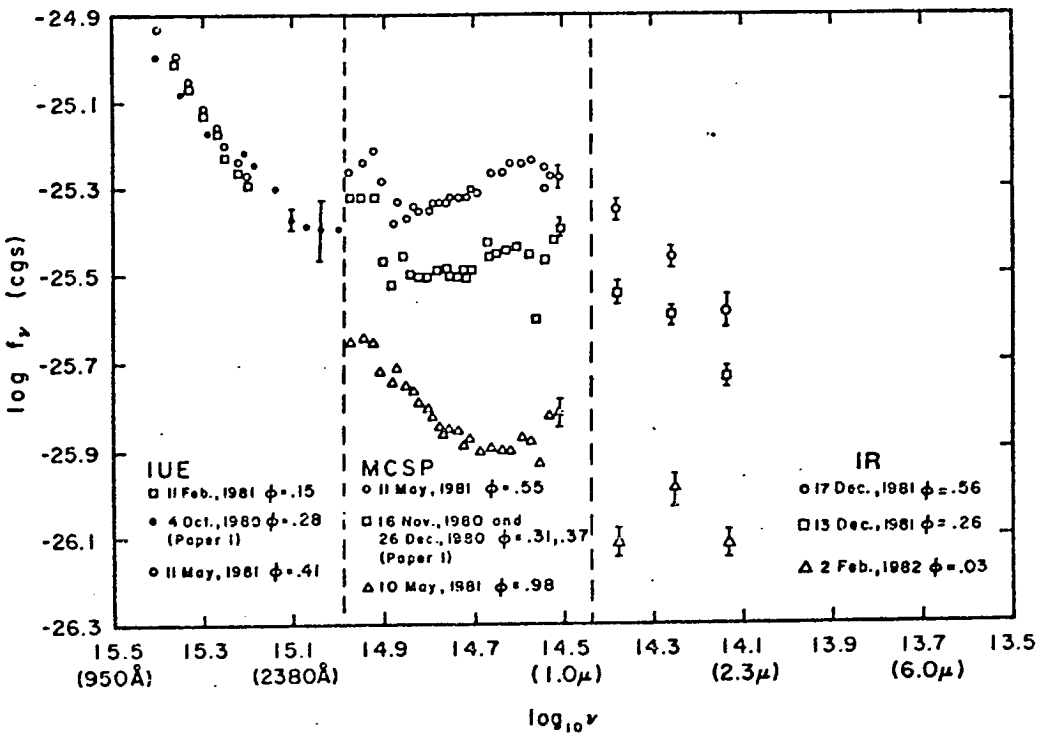

FIG. 2.—Overall energy distribution in the ultraviolet, visual, and infrared frequencies and at various phases, as indicated

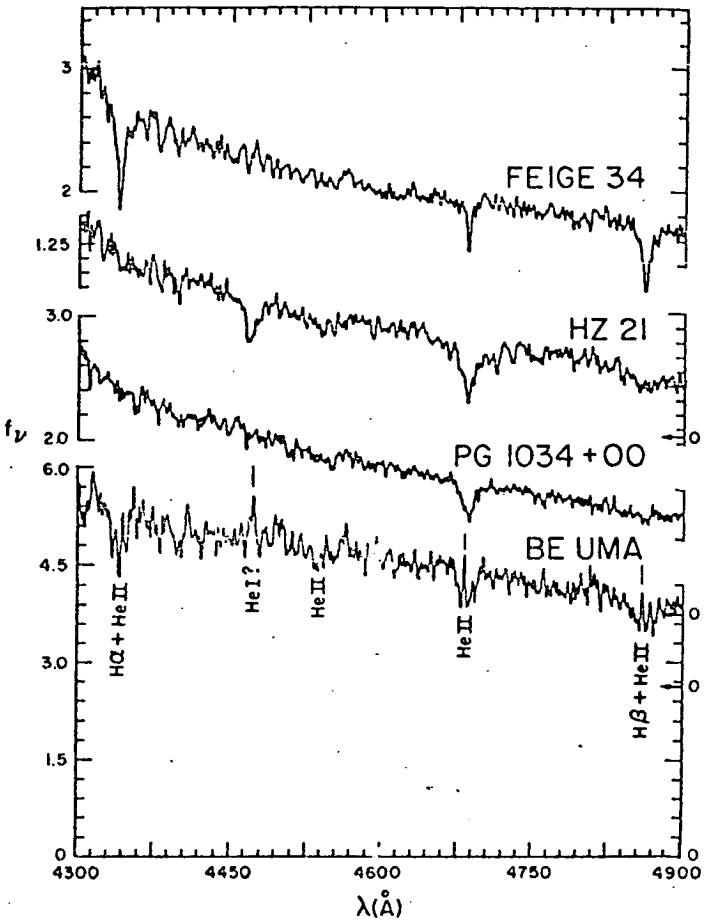

FIG. 3.—MMT high-resolution spectrum of BE UMa near minimum light but outside eclipse (*bottom tracing*) and three comparison stars with helium-rich compositions, but with different temperatures and gravities. The separate spectral traces are offset vertically. All are on linear scales in flux per unit frequency. The scale is shown by numbers on the left-hand axis, and zero points for separate tracings are indicated by arrows on the right-hand axis. Since the use of a narrow entrance slit precludes the obtaining of absolute fluxes, no absolute units are presented. Analysis of the spectrum (see text) shows that the BE UMa primary belongs to the "hot DO" class (WGL), of which PG 1034+001 is representative. Unlike that star, however, BE UMa possesses a barely detectable trace abundance of hydrogen, like the cooler white dwarf HZ 21 and the lower gravity subdwarf Feige 34.

spectrum in isolation just outside of eclipse and detection of the spectrum of the unilluminated side of the secondary star during the eclipse.

Figure 3 shows a blue spectrum dominated by the primary star obtained at phase 0.02–0.03, along with some similar stars of high surface gravity presented for comparison. All spectra were obtained on the same night with the MMT spectrograph and intensified photon-counting Reticon detector (Latham 1979) affording 1.5 Å spectral resolution. The spectra reveal broad absorption lines of Hγ–He II λ4340, He II λ5411, He II λ4686, and Hβ–He II λ4861. Weak, central hydrogen emission cores are evidently due to the residual reprocessing component. Nonetheless, the absorption profiles may be analyzed with model atmospheres calculated to fit high-gravity stars, and this is done in § III. Not shown are spectra of the same four stars covering λλ5100–6600 obtained the same night.

A series of low-dispersion (~10 Å resolution) spectra covering 3300–7000 Å were obtained near and during the eclipse phase 0 with the Steward 2.3 m reflector, Cassegrain spectrograph, and intensified Reticon system. Unfortunately, the use of a blue-sensitive RCA front-end image tube precluded obtaining a high signal-to-noise ratio red spectrum. The top three scans in Figure 4 are consecutive 12 minute exposures during eclipse, though the last includes contamination due to the reemergence of the hot stellar component at the end of the

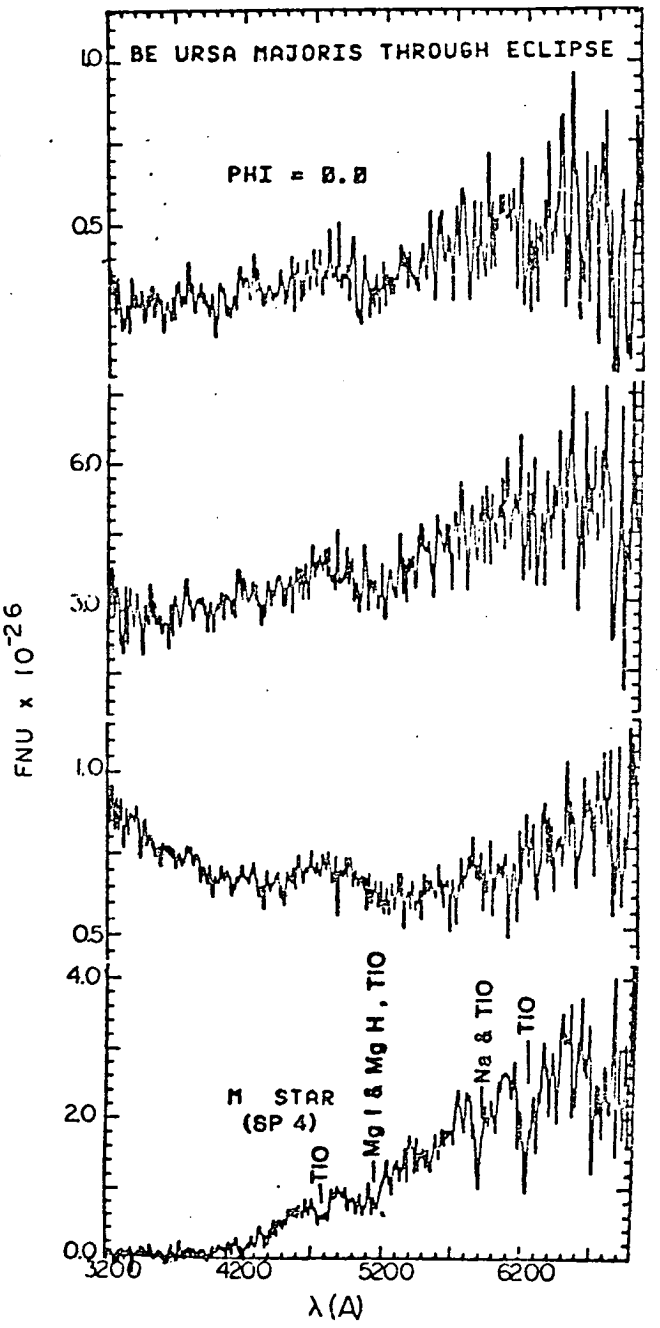

FIG. 4.—Three spectra of BE UMa covering the brief eclipse, obtained in consecutive 12 minute scans. The top scan appears least contaminated by any residual optical radiation from the primary and reprocessing component in the secondary's atmosphere. On the other hand, the hot primary star slope is seen clearly in the third scan from the top. The bottom scan is that of a comparison star, the M-dwarf star SP 4, obtained with the same instrumental configuration.

eclipse. The bottom scan is a comparison dwarf star of spectral type M1 V, cataloged by the name SP 4 (Sanduleak and Pesch 1982), obtained the same night by W. Tifft with the same observing configuration.

Clearly, the top two spectra are dominated by the very red energy distribution of the secondary star, which appears to show the strong Mg I/Mg H λ5200 and TiO λ6200 features typical of an early to middle M dwarf. This confirms the conclusion that the mideclipse V-band light from AON's photometry is dominated by the secondary star. While Hβ is the only weak emission line detected, filling in by Na I emission may weaken the absorption features in the BE UMa M-star component. Comparison with dwarf M spectroscopic standards from Turnshek *et al.* (1985) gives a possible range of M1 V to ~M5 V, the latter extreme requiring the assumption of some residual dilution of the photospheric continuum. The absence of strong CaOH λ5500 and lack of a rapidly rising red continuum preclude a spectral type later than M5. Likewise, the appearance of TiO and absence of strong CN or C_2 bands indicates that the secondary is at least as late as M1, has an oxygen-rich composition, and is not extremely metal-poor. CCH speculated that a λ4050 absorption appearing in their spectrum near minimum light might be due to molecular C_3 absorption originating from a carbon-rich secondary. In fact, their spectrum is clearly dominated at that wavelength by the primary star; it is evident from Figure 2 and this discussion that the secondary contributes less than 10% of the light of the primary at 4050 Å. The unusual strengths of carbon ion transitions in the reprocessing emission spectrum are discussed in § IV*b*, but they probably do not require the assumption of an enriched carbon abundance in the envelope of the secondary star.

e) Lower Dispersion Spectroscopy: The Emission-Line Spectrum of the Reprocessing Component

Additional optical spectra covering 4250–4950 Å and 5100–6600 Å were also obtained at phases other than near minimum in order to study further the reprocessing component. These are discussed extensively by Ferguson (1983) and serve to strengthen and extend certain conclusions from Paper I, MDK, and CCH. Table 4 lists relative fluxes and equivalent widths of lines believed to be reliably detected for three spectra obtained near phase 0.2. In summary, the new data show (1) flat Balmer-line decrements and similar fluxes for He I singlet and triplet lines; (2) prominent lines of moderately high excitation CNO transitions, as well as some possible Fe II identifications; and (3) the weakness or absence of C IV, N IV, and N V lines in the observed wavelength region. The weakness or absence of C IV $\lambda\lambda$5801, 5812, for example, is an important constraint on a line formation model, particularly in light of the strong C III λ4650 blend, as discussed in § IV and Ferguson (1983).

TABLE 4

BE URSAE MAJORIS EMISSION LINE EQUIVALENT WIDTHS NEAR PHASE 0.2 (1981 Jan 9, 10 UT)

Wavelength (Å)	Identification	Flux Relative to Hβ	Equivalent Width (Å)
4340.....	H	1.04	3.78
4380.....	C III	0.17	0.62
4388.....	He I	0.21	0.76
4418.....	N II, Fe III	0.13	0.47
4437.....	He I	0.08	0.29
4471.....	He I	0.17	0.52
4482.....	Mg II	0.15	0.55
4584.....	Fe II	0.05	0.18
4634.....	N III	0.04	0.15
4642.....	N II	0.26	0.94
4650.....	N II, C III	0.61	2.22
4674.....	O II, C III	0.04	0.14
4686.....	He II	0.40	1.45
4707.....	N IV	0.05	0.18
4713.....	He I	0.08	0.29
4861.....	Hβ	1.00	3.63
4921.....	He I	0.40	1.45
4992.....	Fe II	0.18	0.65
5151.....	C II	0.10	0.36
5220.....	Fe II	0.12	0.44
5876.....	He I	0.10	0.36
6347.....	Mg II	0.05	0.18
6563.....	Hα	1.01	3.67
6583.....	N II, C II	0.04	0.15

III. THE BE URSAE MAJORIS COMPONENTS—A REEXAMINATION

a) Parameters of the Primary Star

The form of the primary energy distribution and the photon flux incident at the secondary surface determine the spectrum of the reprocessing component at the secondary. It is essential first to know the primary star temperature T_p and the primary surface gravity g_p. The ranges of possible values derived in previous papers for these two quantities are rather disconcerting: $4 \leq T_p/10^4\ \mathrm{K} \leq 13$ and $6 \leq \log g_p \leq 8$.

The absorption spectrum of BE UMa showing the primary was used to determine T_p and $\log g_p$ independent of any analysis of the light or radial velocity curves. Figure 3 shows the BE UMa spectrum together with those of several other stars discussed in Wesemael, Green, and Liebert (1985, hereafter WGL). For HZ 21, it was found that $T_p = 50{,}000 \pm 3000$ K, $\log g_p \geq 7$, and $\log(\mathrm{He/H}) = 0.5 \pm 0.5$ (see also Koester, Liebert, and Hege 1979), while $T_p = 80{,}000 \pm 20{,}000$ K, $\log g_p \geq 7$, and $\log(\mathrm{He/H}) > 2.0$ were estimated in the case of PG 1034+001. The subdwarf O star Feige 34 with $\log g_p \approx 6$ (Greenstein and Sargent 1974) is also presented for comparison. All the atmospheric parameters were derived from the model spectra of collapsed stars with mixed H and He composition of WGL.

The lack of He I λ4471 in the BE UMa primary spectrum, in contrast to the HZ 21 observation, implies $T_p \geq 65{,}000$ K. On the other hand, T_p cannot be higher than 95,000 K due to (1) the strength of the Brackett He II lines, (2) the significantly greater absorption due to H blended with He II at $\lambda\lambda$4340 and 4861, and (3) the width and strength of He II λ4686. The ultraviolet energy distributions of high-gravity stars with $60{,}000 \leq T_p \leq 100{,}000$ K are so similar that the *IUE* fluxes prove to be a poor temperature discriminant.

Clearly, the Feige 34 absorption lines are narrower than those of the BE UMa primary. The latter's He II absorption line profiles were more consistent with those of PG 1034+001 and marginally narrower than those of HZ 21. For BE UMa, we thus estimate $7.0 \leq \log g_p \leq 8.0$. The greater strengths of Hγ + He II λ4339 and Hβ + He II λ4861 relative to He II $\lambda\lambda$4540 and 5411 indicate that hydrogen absorption is significant, implying an intermediate BE UMa abundance ratio of $\log(\mathrm{He/H}) = 1.0 \pm 1.0$. Thus the BE UMa primary is spectroscopically a DO white dwarf with a helium-rich atmosphere, but with detectable hydrogen; in this it is similar to the "comparison" star HZ 21 (Koester, Liebert, and Hege 1979)

but is unlike most cool DB white dwarfs with nearly pure helium atmospheres.

While the BE UMa primary is a white dwarf according to spectroscopic criteria, note that the indicated surface gravity $\log g_p \gtrsim 7$ agrees with the radius derived by CCH from analysis of the light and radial velocity curves: Assuming a mass $\sim 0.6\ M_\odot$ typical of field white dwarfs, this gravity suggests a radius $\lesssim 3$ times the final radius for a zero-temperature Hamada-Salpeter degenerate star. CCH used the term "subdwarf" for this kind of star. On the other hand, the spectroscopic analysis rules out the $T_p \approx 130{,}000$ K found by CCH from modeling the eclipse light curve. Note that the hottest group of helium-rich pre-white dwarf stars, for which the pulsating PG 1159−035 (GW Vir) is the prototype, is believed to include stars with temperatures in the range 100,000 K and higher. These stars have optical spectra lacking the He II Brackett and H lines but instead show C IV absorption and emission lines; C IV is absent in both the photospheric absorption spectrum and the reprocessing emission spectrum of BE UMa. The high surface gravity derived from the He II absorption line profiles is also inconsistent with the assumption of a main-sequence mass-radius relation for the primary by AON and their consequent finding of a lower effective temperature.

These results do not support the suggestion of Hutchings and Cowley (1985) that the primary star of BE UMa is a pulsating variable star, of the PG 1159−035 type or otherwise. The preceding discussion of the spectroscopic characteristics indicates that the temperature is below that of the PG 1159−035 group. Moreover, the survey work of Grauer *et al.* (1986) found that BE UMa near minimum light—and two other DO white dwarfs of similar temperature—show no evidence for high-frequency photometric variations. Finally, our three *IUE* scans of the 1100–2000 Å region—while limited in comparison to the extensive, time-resolved series obtained by Hutchings and Cowley (1985)—do not support their suggestion that the BE UMa primary star is a large amplitude photometric variable at ultraviolet wavelengths.

b) Constraints from the Observations of the Cool Secondary

In principle the observations of the unilluminated side of the secondary star can be used to estimate reasonable parameters for that star and the system. There may be (at least) three problems with pursuing this hypothesis. First, the fact that the emission lines do not completely disappear during eclipse indicates that some portion of the reprocessed side of the star may still be contributing. That the residual contribution to the continuum is small, however, is indicated by the overall energy distribution of Figure 2 near minimum light. Second, there is a substantial dispersion in the lower main sequence, even for stars of more or less normal (Population I) atmospheric compositions. This leads to an uncertainty of at least 1 mag in the absolute visual magnitude. Third, one must worry about the degree to which the parameters of this component of a close binary, which must be distorted enough in shape to nearly fill its Roche lobe, deviate from those of isolated main-sequence stars. Indeed, CCH argue that the cool component must have a radius too large by a factor of 3 relative to the main sequence. However, the hypothesis of assuming a normal main-sequence secondary star can also be tested by means independent of CCH eclipse-modeling.

The estimates of spectral type within the range M1–M5 V correspond to a wide range of absolute visual magnitude ($9.5 < M_v < 15.2$) but a somewhat narrower range at 2.2 μm ($5.6 < M_K < 8.7$) based on the mean color magnitude relations derived by Probst (1983, Table 3). Indeed the K-magnitude observed at minimum light may be the observed bandpass most dominated by the secondary star, so that component must have $K > 14.7$. The extreme values of M_K quoted above lead to photometric parallaxes (expressed as distances) between 660 pc and 160 pc.

Some discrimination among the range of possible M-dwarf components is possible by comparing the observed color at the two longest wavelengths, $H-K$, with those for M dwarfs. The two observations nearest minimum light (Table 3) at phase 0.03 yield $H-K$ values of +0.17 and +0.16, near the Probst (1983) mean for stars at $M_v \approx +9$ (spectral type M0–M1). Unfortunately, any residual continuum for the reprocessing component will make the measured color bluer, so that the true cool component may be somewhat cooler and lower in the luminosity. Since the minimum light energy distribution shows little indication of a significant contribution from this reprocessed continuum component (Fig. 2), the infrared, on balance, favors a companion closer to the top end of the previously derived range ($M_v \approx +9$–10, near type M1). The implied distance is ~ 600 pc.

This result may now be compared for consistency with the photometric parallax derivable from the fitted atmospheric parameters of the primary star. Nearly degenerate stars at $T \approx 80{,}000$ K should have $+9.5 > M_v > +7.0$, corresponding to the range in surface gravity estimated earlier as $7.0 < \log g < 8.0$. Using the minimum light approximate V mag (16.15) from the MCSP spectrophotometry, the derived range in distance modulus is $6.65 < m-M < 9.15$, or $213 < d < 676$ pc. This falls within the range derived for a photometric parallax of the secondary star. On balance, the preferred distance is probably near the upper bounds for both techniques, some 500–600 pc. This is in nice agreement with the estimate of 600 pc by CCH, in spite of the fact that our results are consistent with a secondary of approximately main-sequence size and luminosity—see the discussion in § IIIc.

A further consistency test is offered from using the orbital period, the radial velocity curve, the eclipse constraint, and the assumption that the secondary star has main-sequence parameters corresponding to those in the range M1 V–M5 V. A minimum primary mass is specified by the CCH mass function $f(M_p) = 0.25\ M_\odot$, and one can easily show that the orbital inclination i must exceed 84°. To better than 1% accuracy, assuming $\sin i = 1$, the mass function and Kepler's law give, respectively,

$$M_p/(1 + M_s/M_p)^2 = 0.25\ M_\odot\ ,$$

$$a^3 = G(M_p + M_s)P^2/4\pi^2\ ,$$

where M_p and M_s are the masses of the primary and secondary stars, a is the orbital semimajor axis, P is the orbital period, and G is the gravitational constant. In Table 5, we present parameters derived for the primary star and orbital separation for an assumed secondary mass. The assumed masses and radii for a secondary star of a given absolute visual magnitude are taken from Veeder (1974). The results require that the white dwarf primary should lie in the mass range 0.5–0.7 $M_\odot$ (cf. CCH). This is close to the mean mass for field white dwarfs (Koester, Schulz, and Weidemann 1979; Shipman 1979), including hot white dwarfs with helium-rich atmospheres (Oke, Weidemann, and Koester 1984).

It is also possible to test the radius and surface gravity of the

TABLE 5

BE URSAE MAJORIS COMPONENT PARAMETERS FOR THE RANGE OF POSSIBLE SECONDARY TYPES

Spectral Type	M_s ($M_\odot$)	M_v(sec) (mag)	R_s ($R_\odot$)	$(m-M)_v$(sec) (mag)	Distance (pc)	a ($R_\odot$)	M_p ($M_\odot$)	log g_p
M1 V.....	0.47	9.0	0.63	8.3	460	7.7	0.70	7.5
M5 V.....	0.21	11.8	0.32	5.5	130	6.5	0.50	8.5

primary, as a check of the analysis of the photospheric spectrum. Again using the distance moduli assignable to main-sequence secondaries within the allowed range, a corresponding range in absolute magnitude M_v for the primary is determined, since the apparent magnitude of this component is known ($V = 16.15$). Now a comparison of the high-temperature/high-gravity model sets for both helium and hydrogen-rich compositions (Wesemael *et al.* 1980; Wesemael 1981; WGL) shows that M_v or just the Eddington flux at 5500 Å is insensitive to temperature and composition in the range 65,000–95,000 K allowed by the model atmosphere analysis; instead the major dependence is on gravity. Hence, we can calculate the radius of the primary R_p from the surface area necessary to match the M_v corresponding to a given secondary type and distance. The corresponding log g can be determined, since the dynamical arguments specify a primary mass for a given secondary type. The results, $7.5 \leq \log g \leq 8.5$, is again consistent with the photospheric gravity determination (from the absorption line widths) and with the conclusion that the primary star in BE UMa is a hot DO white dwarf. Further discrimination is possible because theoretical calculations also specify a mass-radius (gravity) relation for white dwarfs. The recent finite-temperature calculations applicable to such a hot white dwarf (cf. Koester and Schönberner 1986) predict modestly smaller gravities ($\log g \approx 7.8$ vs. 8.0) for a star near 80,000 K than does the zero-temperature Hamada Salpeter relation (for a carbon-oxygen core composition). For the primary mass range near $0.6 \pm 0.1\ M_\odot$, the surface gravity, therefore, cannot exceed $\log g = 8$. This in turn suggests that the correct secondary stellar mass should be near the high end of the range, corresponding to an earlier spectral type.

c) *Constraints from the Eclipse Light Curve*

Our analysis of the spectra and the energy distributions of both stellar components results in some parameters consistent with the analysis of CCH; however, parameters which are inconsistent include the temperature of the primary star and the radius and luminosity of the secondary star, which they called a "subgiant." We compare first the analyses of the secondary star.

Our photometric parallax estimate based on the minimum K(2.2 μm)-magnitude suggests a secondary star of early M spectral type having a radius and luminosity near the corresponding main-sequence values. CCH, on the other hand, estimate its radius at $\sim 2 \pm 0.4\ R_\odot$ (vs. $\sim 0.5\ R_\odot$, for the main sequence). This value requires that the object be ~ 2 mag overluminous at 2.2 μm, compared to main-sequence early-M dwarfs (or even more overluminous for a late-M dwarf). For an assumed $M_K \approx +3$ of a subgiant, the observational constraint that this component has $K > 14.7$ (§ III*b*) yields a lower limit to the distance of 2200 pc. This distance implies that the primary star would have $M_v \approx +4.5$, quite inconsistent with the surface gravity inferred from the photospheric analysis.

CCH nonetheless derived a photometric parallax from the V light attributed to an overluminous secondary star consistent with a distance of ~ 600 pc, a value which is compatible with the other considerations. How was this possible? The answer lies in their interpretation of the photometry of AON, who made the stunning discovery of the brief eclipse. It is likely from the discussion by AON that the observations near eclipse minimum were sky-limited, especially in the V-band (their channel 5). CCH interpreted the noisy "bottom" of the V curve to be limited by the V-brightness of the secondary star, rather than by the sky. (Note that the U curve, where the relative sky contribution is much less important, reached no flat-bottomed minimum.) We contend that the secondary star is actually much less luminous at V, although we can provide no accurate minimum V-flux from the contaminated slit spectrophotometry presented in § III*b*.

A second aspect of the inferences from the eclipse photometry was the interpretation of the time durations between contact points. The long eclipse ingress and egress ($\gtrsim 0.005$ of the binary period) are potentially at variance with the inferred (small) size of the primary star. CCH found that the inclination angle of the orbit must be significantly less than 90° so that the eclipse could be grazing, and the occulted hot star could approach the dimensions of a white dwarf. We concur with this argument. However, since they interpreted the V-minimum as a detection of the secondary star, the length of time between contact points 2 and 3 then forced this component to be extremely large. We argue that the true total eclipse by the secondary is likely to be shorter and at a fainter (as yet undetected) magnitude level. The proper constraint imposed by the eclipse can only be obtained by more accurate eclipse photometry, especially at longer wavelengths, where the contribution of the uneclipsed primary limb is less important.

It is difficult to assess why the eclipse modeling yielded a much hotter temperature for the white dwarf primary star than is consistent with that component's spectrum. We have not attempted to model the published light curves with a program similar to that used by CCH. However, it may be relevant to note that the energy distributions of hot white dwarfs differ greatly from those of blackbodies, and the effective temperatures differ greatly from the blackbody temperatures. Moreover, one may cite examples in the literature, such as Hills (1971) light curve analysis of V471 Tauri = BD +16°516B, in which the inferred temperature of a hot white dwarf is much higher than the temperature later derived from model atmosphere–fitting. Finally, it would be useful to obtain additional multiwavelength photometry, covering the eclipse accurately at high time resolution, as a prelude to further analysis of these stellar parameters.

IV. THE REPROCESSED RADIATION SPECTRUM

Models for the emergent energy distribution of an 80,000 K DO white dwarf indicate that the primary bathes the second-

ary with a radiation field which peaks in the extreme-ultraviolet (EUV) wavelength region; the flux should drop markedly shortward of the He II λ228 "Lyman" edge. This ultraviolet radiation should be reprocessed into line and continuum radiation, a large fraction of which emerges at optical wavelengths, as we shall discuss. The outer atmosphere of the secondary on the hemisphere facing the primary star exhibits characteristics analogous to chromospheres, but of course the method of energy deposition is completely different: a high-temperature radiation field from an external source. Ferguson (1983, and in preparation) has performed exploratory modeling which attempts to define the physical parameters for different layer depths in the secondary's envelope. In the following, we describe some of the qualitative results.

a) The Continuum

Sufficient ultraviolet radiation is intercepted by the secondary to account for the unique observed reflection effect, as we show in this section. The large amplitude of the Balmer jump in emission shows that the reprocessed component is formed largely from hydrogen bound-free radiation. The resulting energy distribution can then be approximated as a blackbody with temperature T_{rep} derived (via the Wien law) from the maximum near 7500 Å of the reprocessed component—see Figure 2. Despite the effect of the Paschen edge on this determination based on low resolution spectrophotometry, it is at least clear that the Planckian peak of the reprocessing component occurs within the range 6–10,000 Å. This corresponds to $T_{rep} \sim 6500^{+2000}_{-1400}$ K. Equating the total integrated flux of the reprocessed component to the fraction of the primary radiation intercepted by the secondary, we can estimate the size of the primary star or its surface gravity log g_p via the following relations:

$$R_p = 2a(T_{rep}/T_p)^2$$

or

$$\log g_p = \log \{GM_p/[2a(T_{rep}/T_p)^2]^2\} .$$

Assuming a binary separation of 7.4 $R_\odot$, a primary mass of 0.64 $M_\odot$, and primary temperature of 100,000 K, we derive $7.3 < \log g_p < 8.2$. The range corresponds to that for the values of T_{rep}. If instead we assume a more realistic primary temperature of 80,000 K, the procedure yields $6.9 < \log g_p < 7.8$, in line with our other estimates. Moreover, a temperature of at least 80,000 K is required from this measure of the energy balance at the secondary star.

b) The Emission-Line Spectrum

Extreme-ultraviolet (100–1000 Å) radiation is absorbed in the atmosphere of the secondary and converted to optical continuum radiation at a physical depth where the optical depth of the secondary's atmosphere τ_{EUV} is on the order of unity. The layers above this physical depth in the secondary's atmosphere will be highly ionized in a Strömgren sphere–like fashion.

An estimate of the electron density n_e at the optical depth of hydrogen line formation is available using the Inglis-Teller relation. Spectra show that H14 is the unresolved emission line closest to the Balmer jump, so that

$$n_e < 2 \times 10^{14} \text{ cm}^{-3}$$

Ferguson (1983) discussed high-resolution echelle spectroscopy defining the profiles of the Hβ λ4861, He II λ4686 and C III λ4650 emission lines. Hβ presented the broadest profiles, which a full width at half-maximum (FWHM) of the emission at 240 km s^{-1} at all phases. The He II λ4686 FWHM was 48 km s^{-1}. Both Hβ and He II showed absorption cores at phases 0.84 and 0.15, giving the appearance of the doubled emission lines reported by CCH; these authors also reported that the absorption dips reached phase 0.15, the absorption core disappeared in Hβ, but the weaker He II line was poorly measured at that phase. The narrow FWHM of the C III λ4650 blend shows that the widths of the Hβ and He II lines are due to optical depth effects, not to rotation of the secondary. These findings suggest that the hydrogen Balmer series is found deep in the reprocessing envelope, perhaps coincident with the non-LTE reprocessed continuum. The flat Balmer decrement requires that electron temperatures in the hydrogen line formation region exceed 10,000 K.

The rather flat He I decrement indicates that the $2p^3P^o$ and $2p^1P^o$ terms are radiatively populated as with hydrogen. The He I line formation zone is thus likely to be very near to or coincident with the hydrogen line formation region.

Ferguson (1983) resolved the C III λ4650 blend into its triplet constituents; however, the components remained unresolved in velocity at 0.15 Å resolution, showing that the rotation rate of the secondary star does not much exceed 10 km s^{-1}. Their much lower optical depths suggest that these lines are formed above the hydrogen line–producing zone.

The EUV continuum from the primary star is bright enough to excite fluorescent emission in the secondary's atmosphere. Excitation occurs above the hydrogen recombination zone, where the remaining electrons in highly ionized species are excited by the continuum radiation, and some fraction decay via optical transitions (Williams and Ferguson 1982, hereafter WF). The line spectrum produced by this "continuum fluorescence" (CF) mechanism is different from the normal optical spectrum produced by the ions because the strong ultraviolet pumping line represents the normal decay route of these levels, and the optical transitions would not be observed in the absence of ultraviolet radiation. A "feed" line occurs when several ultraviolet transitions populate a single optical transition. Feed lines typically require excitation photons of ~350 Å, redward of the He II λ228 edge. Table 6 shows observable fluorescence transitions and their excitation wavelengths (WF). The presence of the fluorescent process in BE UMa is verified by the pure CF lines N II λ4640 and O III λλ5268, 5508. The strength of C III λ4650 in the reprocessing spectrum is probably also due to the CF mechanism, as WF argued in application to cataclysmic variable spectra.

The primary's EUV energy distribution, which determines the fluorescence spectrum, is controlled by the temperature and helium abundance of the primary's photosphere. Energy distributions for pure helium, high-gravity atmosphere models (Wesemael 1981) were examined to see at what temperatures EUV radiation at various feed lines becomes significant. The models show that significant continuum flux at the necessary wavelengths begins to appear at 80,000 K and increases with higher temperatures. This lower limit on the primary star temperature is consistent with our determination above.

The incident radiation for an 80,000 K helium-rich star declines rapidly shortward of He II Lyβ near 259 Å, the C III ionization limit (see, for example, the synthetic spectra of WGL). We would therefore expect that any C III recombination spectrum should be weak; note that the low-lying C IV λλ5801, 5812 doublet is not detected in the reprocessing emis-

TABLE 6

METAL CONTINUUM FLUORESCENCE LINES

Species	Wavelength (Å)	Resonance Wavelength (Å)	Term	Equivalent Width* (Å)
C IV	5805	312	$2s^2S-3s^2S-3p^2p^o$	>5.4
C III	5250	291	$2s^1S-5p^1P^o-4d^1D$	N
	5483	274	$2s^1S-6p^1P^o-5d^1D$	?
	4255–4258	341	$2p^3P^o-5d^3D-4d^3D$	Y
	4378–4388	Feed	$5p^3P^o-4d^3D$	Y
	4515–4516	348	$2p^3P^o-5s^3S-4p^3P^o$	0.15
	4647–4651	Feed	$3p^3P^o-3s^3S$	Y
	4672–4673	319	$2p^3P^o-7d^3D-5p^3P^o$	Y
	5159–5161	321	$2p^3P^o-7s^3S-5p^3P^o$	?
	5409–5410	319	$2p^3P^o-7d^3D-5f3F^o$	?
N III	4098	Feed	$2s3p^2P^o-2s3s^2S$	?
	4543	300	$2s2p^2P^o-2s5s^2S-2s4p^2P^o$	?
	4640	374	$2s2p^2P^o-2p3d^2D-2s3p^2P^o$	0.51
	4818	315	$2s2p^2P^o-2p3d^2D^o-2p3p^2P$	Y
	6515	306	$2s2p^2P^o-2s3p^2S-2s4p^2P^o$	0.34
	4511–4535	396	$2p^4P-3p^4D-3s^4P^o$	N
	5261–5314	358	$2p^4P-3d^4P^o-3p^4P$	N
O III	5268	320	$2p^1D-3d^1P^o-3p^1S$	0.86
	5508	328	$2p^1D-3d^1D^o-3p^1D$	1.01
	5592	Feed	$3s^1p^o-3p^1P$	Y

* N, not detected; Y, feature detected in emission, but not measured well enough for an equivalent width to be estimated (see Ferguson 1983).

sion spectrum. Table 5 shows that several C III triplet groups, including the prominent λ4650 blend, are observed. Higher energy levels that can feed these transitions can be populated from excitation by the numerous continuum photons longward of 300 Å. In fact, the λ4650 transitions are the only outlet for radiative deexcitation of the $3p^3P^o$ level and have a large combined log $gf \sim 0.3$.

The weakness of corresponding C III singlet transitions such as λ5250 and λ5483 is more difficult to understand; the CF process should originate by photons exciting electrons out of the ground states. Since the singlet ground state lies 6.5 eV lower than the triplet ground state, the Boltzmann factor certainly favors the former. The presence of the triplet emission implies a lower limit T_e of 2×10^4 K in order to populate the triplet ground state level to even a few per cent of the singlet ground state level. However, most singlet feeder levels may require excitation by photons shorter in wavelength, where the stellar flux is strongly attenuated by He II lines. The absence of well-determined transition probabilities for most transitions of interest precludes a more quantitative evaluation. Certainly, the triplet transitions are generally more numerous and stronger than the singlets.

The He II emission spectrum ought to be weak for the same reason that the C IV is weak: there are few stellar photons below 227 Å. It is interesting to note that the weak He II lines are more recombinational in their decrement and considerably narrower. It is possible that the CF mechanism plays a role in the relative strength of He II λ4686 observed in BE UMa.

c) *Other Systems Similar to BE Ursae Majoris*

As other detached binaries are known with similar periods and also involving a very hot primary star, it is worthwhile to contrast the differences which make the spectrum of reprocessed radiation from BE UMa unique. The two most similar systems involving hot white dwarfs are probably Feige 24 (see also MDK) and GK Vir (PG 1403+01).

While the Feige 24 system is not an eclipsing binary, it is enough inclined that the visible H and He I emission lines are modulated in phase over the system's 4.2 day period, indicating a reflection effect similar to that seen in BE UMa, although of lower excitation (Thorstensen *et al.* 1978). The peak Hα equivalent width is 2.6 Å with a recombinational Balmer decrement, although a blue continuum contribution might mask the higher Balmer series line emission. Liebert and Margon (1977) found a ratio of equivalent widths of He I λ6678 to Hα of ~0.16, while Ca II λ3933 reached about half the equivalent width of Hε near the maximum in emission-line strengths. These authors also found the secondary to be an M1–M2 V star, consistent with its having main-sequence parameters. Analysis of the primary star suggests $T_p \approx 55{,}000$ K (Holberg, Wesemael, and Basile 1986) or $T_e \approx 63{,}000$ K (Wesselius and Koester 1978). Thus, Feige 24 exhibits a much less spectacular reflection effect than BE UMa, since (1) the temperature of the primary is substantially lower and (2) its DA composition means that EUV radiation shortward of the (hydrogen) Lyman limit is largely extinguished in the emergent spectrum. Our calculations, assuming a separation of 11 $R_\odot$, suggest a reprocessing temperature T_{rep} at the secondary of less than 1500 K.

GK Vir (Green, Richstone, and Schmidt 1978) also has a substantially shorter period and is in addition an eclipsing system. The derived range of solid angles subtended by the secondary and orbital separations are favorable to a strong reprocessing spectrum. However, the physical parameters for both the primary and secondary are not well determined: the primary star is clearly a hot DA white dwarf, but it is not established that it is as hot as the BE UMa primary. The barely detected secondary could be very late (see Green, Richstone, and Schmidt 1978). No reprocessing component is detected outside of eclipse, and the flux from residual reprocessing plus secondary star is observed to be at least 5 mag fainter than the primary in visual light during eclipse. Since the orbital separation for GK Vir is ~3 times smaller than that of BE UMa, we

must infer that (1) the secondary is considerably smaller in GK Vir, or (2) the primary produces much less EUV flux at the secondary surface, or both.

d) Summary

The reprocessing component is caused by photoionization of the secondary by the primary. The outermost secondary atmosphere is highly ionized, containing He II, C IV, O III, N III, and perhaps N IV. Metal recombination and CF line formation occurs in these outermost regions where the minimum electron temperature is 20,000 K. The λ4650 C III blend is produced by CF. Hydrogen Balmer emission and the bound-free optical continuum are produced somewhat deeper in the BE UMa atmosphere where the electron temperature exceeds 10,000 K and electron densities are $\sim 10^{14}$ cm^{-3}.

V. CONCLUSIONS

BE Ursae Majoris is of particular physical interest because of its unusually strong, high-excitation reflection effect, arising from EUV irradiation of the cool secondary star by the hot, compact primary. Analysis of a variety of new observations provides a self-consistent physical picture of the system. The primary is a DO white dwarf, with an effective temperature of 80,000 $\pm$ 15,000 K, a surface gravity log $g > 7.0$, and a surface composition of mixed helium and hydrogen with log (He/H) = 1.0 $\pm$ 1.0 by number. Such a star will have substantial emergent EUV flux longward of the He II ionization edge of 227 Å. From the orbital characteristics and the assumption that the secondary obeys a normal main-sequence mass-radius relation, the primary mass is found to be 0.6 $\pm$ 0.1 $M_\odot$. The radius is then consistent with theoretical cooling curves at $\sim$1.4 times the zero-temperature radius for degenerate matter. No evidence is found in this study for variability of the primary.

The main-sequence secondary star is of early-M spectral type; a formal range of M1–M5 is possible, with the probable value near the early end. The distance follows from the photometric parallax of both stars; it is around 600 pc, which yields an orbital separation of $\sim 8\ R_\odot$. The irradiation of the photosphere of the secondary raises the effective temperature of the side facing the primary to 5000–8500 K. A strong, high-excitation emission-line spectrum from species such as He I, C III, O III and N III is formed from recombination and continuum fluorescence. In addition, the spectra exhibit a flat Balmer decrement, a large Balmer jump in emission, and a flat decrement of He I lines with similar singlet and triplet line strengths. These lines must be formed at greater depth than the high-excitation lines in the envelope, in a region with $T_e > 10{,}000$ K and $n_e \approx 10^{14}$ cm^{-3}. The striking resemblance of this emission spectrum to those of some high-excitation cataclysmic variables suggests that a detailed understanding of the EUV irradiation processes in the photospheric plasma of the secondary in BE UMa will have a direct bearing on the interpretation of accretion disk spectra.

We are grateful to W. Tifft for donating observing time for the secondary optical spectra near minimum light and to R. Williams for useful discussions. This work was supported in part by NSF grants AST-8024324 and AST-8514778 and NASA grant NAG5-38 to the University of Arizona.

REFERENCES

Ando, H., Okazaki, A., and Nishimura, S. 1982, *Pub. Astr. Soc. Japan*, **34**, 141 (AON).
Cox, J. P., and Giuli, R. T. 1961, *Ap. J.*, **133**, 755.
Crampton, D., Cowley, A. P., and Hutchings, J. B. 1983, *Ap. J.*, **272**, 202 (CCH).
Elias, J. H., Frogel, J. A., Matthews, K., and Neugebauer, G. 1982, *A.J.*, **87**, 1029.
Ferguson, D. H. 1981, unpublished.
———. 1983, Ph.D. thesis, University of Arizona.
Ferguson, D. H., Liebert, J., Green, R. F., McGraw, J. T., and Spinrad, H. 1981, *Ap. J.*, **251**, 205 (Paper I).
Grauer, A. D., Bond, H. E., Liebert, J., Fleming, T., and Green, R. F. 1986, *Ap. J.*, submitted.
Green, R. F., Richstone, D. O., and Schmidt, M. 1978, *Ap. J.*, **224**, 892.
Greenstein, J. L., and Sargent, A. I. 1974, *Ap. J. Suppl.*, **28**, 157.
Hills, J. G. 1971, *Pub. A.S.P.*, **83**, 81.
Holberg, J., Wesemael, F., and Basile, J. 1986, *Ap. J.*, **306**, 629.
Hutchings, J. B., and Cowley, A. P. 1985, *Pub. A.S.P.*, **97**, 328.
Koester, D., Liebert, J., and Hege, E. K. 1979, *Astr. Ap.*, **71**, 163.
Koester, D., and Schönberner, D. 1986, *Astr. Ap.*, **154**, 125.
Koester, D., Schulz, H., and Weidemann, V. 1979, *Astr. Ap.*, **76**, 262.
Kurochkin, N. E. 1964, *Perem. Zvezdy*, Vol. **15**, No. 1, p. 7.
———. 1971, *Perem. Zvezdy*, **18**, 85.
Latham, D. W. 1979, *Smithsonian Ap. Obs. Spec. Rept.*, No. 385, p. 119.
Liebert, J., and Margon, B. 1977, *Ap. J.*, **216**, 18.
Liller, M. H., and Liller, W. 1975, *Ap. J. (Letters)*, **199**, L133.
Margon, B., Downes, R. A., and Katz, J. I. 1981, *Nature*, **293**, 200 (MDK).
Neugebauer, G., Oke, J. B., Becklin, E. E., and Matthews, K. 1979, *Ap. J.*, **230**, 79.
Oke, J. B., Weidemann, V., and Koester, D. 1984, *Ap. J.*, **281**, 276.
Probst, R. 1983, *Ap. J. Suppl.*, **53**, 335.
Sanduleak, N., and Pesch, P. 1982, *Ap. J. (Letters)*, **258**, L11.
Shipman, H. 1979, *Ap. J.*, **228**, 240.
Thorstensen, J. R., Charles, P. A., Margon, B., and Bowyer, S. 1978, *Ap. J.*, **223**, 260.
Turnshek, D., Turnshek, D. A., Craine, E., and Boeshaar, P. 1985, *Atlas of Digital Spectra of Cool Stars* (Tucson: Western Research Company).
Veeder, G. J. 1974, *A.J.*, **79**, 1056.
Wesemael, F. 1981, *Ap. J. Suppl.*, **45**, 177.
Wesemael, F., Auer, L. H., Van Horn, H. M., and Savedoff, M. P. 1980, *Ap. J. Suppl.*, **43**, 159.
Wesemael, F., Green, R. F., and Liebert, J. 1985, *Ap. J. Suppl.*, **58**, 379 (WGL).
Wesselius, P. R., and Koester, D. 1978, *Astr. Ap.*, **70**, 745.
Williams, R. E., and Ferguson, D. H. 1982, in *IAU Colloquium 72, Cataclysmic Variables and Related Objects*, ed. M. Livio and G. Shaviv (Dordrecht: Reidel), p. 97 (WF).

ROC CUTRI and JAMES LIEBERT: Steward Observatory, University of Arizona, Tucson, AZ 85721

DONALD H. FERGUSON: Lockheed Missiles and Space Company, Inc., 1111 Lockheed Way, Building 579, Mail Code 64-23, Sunnyvale, CA 94086

RICHARD F. GREEN: Kitt Peak National Observatory, National Optical Astronomy Observatories, P.O. Box 26732, Tucson, AZ 85726

JOÃO E. STEINER: Instituto de Pesquisas Espaciais, Av. dos Astronautas, 1758, Caixa Postal 515, São Jose dos Campos, S.P., Brazil

SUSAN TOKARZ and S. P. WILLNER: Center for Astrophysics, 60 Garden Street, Cambridge, MA 02138